UNCERTAINTIES IN LIQUID METAL FUSION BLANKET DESIGN WINDOWS

James K. Garner
TRW Inc.
One Space Park, R1/1078
Redondo Beach, CA 90278
(213) 536-1388

Mohamed A. Abdou
School of Engineering and Applied Sciences
University of California, Los Angeles
Los Angeles, CA 90024
(213) 206-0501

ABSTRACT

The work reported here attempts to: 1) define limits for the design windows for liquid metal breeders and coolants with various structural materials in various tokamak fusion reactors, and 2) quantify the impact of uncertainties in these limits on the design window. MHD pressure drop and heat transfer models are developed and used to quantify the effects of varying several tokamak reactor and blanket design parameters and materials properties. Uncertainties in the present pressure drop equations and calculational methods are also considered. Calculations are used to evaluate the impact of the coolant inlet temperature on the thermal cycle efficiency.

An evaluation of the limits of uncertainty gives results ranging from a promising blanket candidate to a severely restricted design window, that would probably exclude self-cooled liquid metal blankets for large tokamaks from consideration. The major uncertainties in the design window result from the current lack of understanding of pressure drop and heat transfer in strong magnetic fields.

INTRODUCTION

Lithium and lead-lithium (17Li-83Pb) cooled fusion blankets offer the promise of excellent neutronic performance, high fusion to electrical energy conversion efficiency, and design simplicity. However, interactive effects such as magneto-hydrodynamic (MHD) pressure drop, flow distribution, heat transfer, corrosion and stress appear to have large enough uncertainties to make the presence of a useful design window questionable, especially in large tokamak reactors.

Table 1 lists reactor, blanket design and materials properties that effect the design window. The nominal values listed in Table 1 are used in all calculations unless stated otherwise. Sensitivity to these parameters is explored in Reference 1 and summarized here. Work has concentrated on the tokamak inboard leg because this is the most difficult area to cool with liquid metals in currently envisioned power reactors. Blanket geometry is also a major factor in the design window. The calculations are generally based on the Blanket Comparison and Selection Study[2] (BCSS) poloidal/toroidal flow blanket geometry, but are intended to be as generic as possible.

Table 1. Liquid Lithium Cooled Tokamak Inboard Blanket Parameters and Nominal Values

REACTOR PARAMETERS	
Maximum magnetic field strength in the blanket (T)	7.2
Heated flow path length (m)	6.45
Neutron wall loading (MW/m^2)	5
First wall heat flux (MW/m^2)	1
BLANKET DESIGN PARAMETERS	
Blanket thickness (m)	0.6
Wall thickness at inlet (cm)	1.5
MATERIALS PARAMETERS (Lithium and Vanadium)	
Maximum interface temperature (K)	1023
Maximum structure temperature (K)	973
Minimum coolant temperature (K)	523
Coolant electrical conductivity (1/ohm m)	1.446e6
Structure electrical conductivity (1/ohm m)	1.8e6
Maximum allowable primary stress (MPa)	125
Coolant density (kg/m^3)	470
Coolant heat capacity (J/kgK)	4180
Coolant thermal conductivity (W/mK)	50

INBOARD TOKAMAK PRESSURE DROP MODEL

A model that can provide useful information about variations in the parameters listed in Table 1, for both lithium and lead-lithium and various structural materials, is described here. The model includes sources of pressure loss in the form of inlet and outlet ducts and turns, and a tapered poloidal channel wall (See Fig. 1). Tapering the conducting channel wall is possible because the pressure, and therefore the primary stress, is significantly lower at the channel

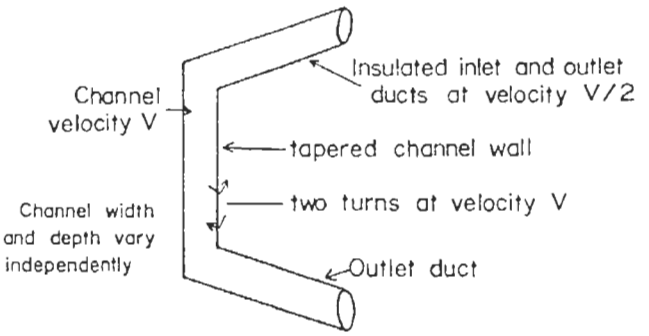

Figure 1. MHD Pressure Drop Model

outlet than at the inlet. The thinner wall over part of the flow path length results in a lower total pressure loss. This concept was utilized in BCSS.[2,3]

The inlet and outlet channels are assumed to be circular insulated ducts lined with 1 mm of the blanket structural material. The coolant velocity in the ducts is taken as half that in the poloidal channels, based on the assumption that there is more space available for the inlet and outlet ducts. The insulation is not in a region of high neutron flux, and can be loaded entirely in compression by surrounding the channel with a thick structural wall. This approach has been taken in several blanket design studies.[3,4,5,6]

Two turns, with a velocity equal to that of the poloidal channels, are included for getting the coolant up to and away from the first wall. Only turns with one leg parallel and one leg perpendicular to the magnetic field are assumed to incur pressure losses. No contractions or expansions have been included. (Contractions and expansions are discussed below). This model is intended to be optimistic, but not overly so.

The model desribed here is similar to, and yields results consistent with, the one used for the toroidal/poloidal flow blanket design in BCSS[2,3]. However, the components of the model (two turns, insulated inlet/outlet ducts, and a large poloidal channel with tapering walls) are general in nature for liquid metal blankets on the inboard side of a tokamak. In our opinion, these components comprise the minimum feasible requirements for cooling the blanket. It is likely that adequate cooling will require more front-to-back circulation in the poloidal channels than has been accounted for in the model, and since the liquid metal must travel perpendicularly to the magnetic field to achieve this circulation, pressure drops are likely to be higher than those reported here. Barring innovations such as electrical insulation materials that will operate in the fusion environment, this model is expected to give a lower bound on pressure drop.

The inlet/outlet duct pressure drop is found by integrating the Hartmann equation,[4] assuming that the magnetic field strength is inversly proportional to the distance from the axis of revolution of the torus, assuming that the flow path is perpendicular to this axis, and that the conducting wall is thin. The BCSS[2,3] values of 36 T at the axis of the torus and a 5 m major radius are used in the calculations unless otherwise specified. The inlet/outlet pressure drop is directly proportional to the wall thickness. If the insulated wall concept cannot be made to work, and the required wall thickness were 2 cm, the inlet/outlet pressure would be on the order of 40 percent of the total drop, rather than on the order of 2% as it is in our model.

The equation used for turns with one leg perpendicular and one leg parallel to the magnetic field is:

$$1)\ \Delta P = V\sigma B^2 a \sqrt{c}$$

where

V = velocity

σ = coolant electrical conductivity

B = magnetic field strength

a = channel half width parallel to the field

$c = \sigma_w t/\sigma a$

σ_w = wall electrical conductivity

t = wall thickness

This equation is a conservative interpretation of limited empirical data,[6,7] and has been used in blanket design studies.[3,4,5]

Tapered Conducting Wall Thickness

The conducting wall in the poloidal channel is assumed to vary linearly over the channel length. The pressure drop is found by integrating the Hartmann equation over the channel length with a linear wall thickness:

$$2)\ \Delta P = \int_0^L B^2 V\sigma \frac{(mx + b)}{(1 + mx + b)}\, dx$$

$$= B^2 V\sigma \left[L - \frac{1}{m} \ln \frac{ML + b + 1}{b + 1} \right]$$

where

$mx + b = c$ ($c = \sigma_w t/a$ as above)

$t = x + \beta$ is the linearly varying wall thickness

(σ and β are constants)

$m = \sigma_w \alpha/\sigma a$

$b = \sigma_w \beta/\sigma a$

Note: $x = 0$ at the channel outlet since ΔP is taken as the pressure increases along path L.

It has been shown[8] that changes in magnetic field and channel size can result in local eddy currents, and therefore increased pressure drops. Equation 2 could grossly underestimate pressure drop in a channel with tapering walls if such eddy currents occur. Since the wall taper is gradual (approximately 12 mm change over a 6 m path for most of the cases analyzed below), eddy currents analogous to those found in abrupt changes in field strength, and relatively abrupt changes in channel size, may not be a problem. Abrupt stepwise changes (which are easier to manufacture) would seem to be more likely to result in eddy currents, but the amount of tolerable change is unknown. The consequences of such eddy currents also have not been quantified.

Assuming that a continuously tapered first wall is feasible, and that Equation 2 correctly models the pressure drop, it is possible to optimize the amount of wall taper to minimize pressure drop as constrained by primary stress. An iterative method, has been used to find the optimum linear taper and the pressure and stress limits of the design window. Values used for reactor and blanket design parameters are taken from Reference 2, and are shown in Table I. The poloidal channel width is 22.5 cm unless otherwise stated.

Constant Thickness Versus Tapered Wall Results

Figure 2 shows the design window resulting from the pressure drop model and compares it with a constant thickness wall design. The design window is defined by temperature and stress limits. The ordinant is the blanket outlet temperature, assuming an inlet temperature of 573 K. The abcissa is the neutron wall loading. The first wall heat flux and heat deposition within the blanket are both proportional to the first wall neutron loading, thus making wall loading a measure of the total thermal power.

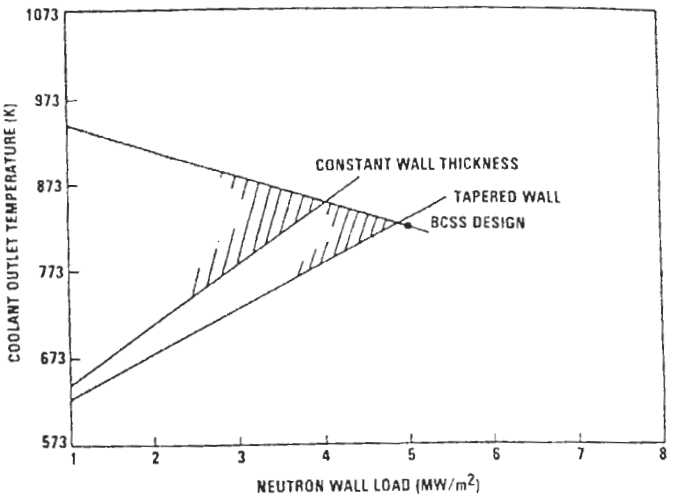

Figure 2. Tapered Wall and Constant Thickness Wall Design Windows. (300°C inlet temperature.)

Possible designs must fall below the temperature line (the upper line), and above the stress line (lower line) in Fig. 2. The temperature limit (top line) is determined by subtracting the film temperature drop plus the temperature drop through the first wall from the maximum allowable structure temperature. The line slopes downward with increasing wall loading because the film temperature drop and first wall drop increase in direct proportion with the first wall heat flux, which increases proportionally with wall loading. The slope of the line is found by assuming a 100 K film temperature drop and a 50 K first wall drop at a neutron wall load of 5 MW/m^2 and a first wall heat flux of 1 MW/m^2. These temperature drop values are based on results from recent design studies, and are discussed further below.

The stress limit (lower line) increases with wall loading because more heat must be removed, requiring a higher flow rate (which results in higher stress and more pumping power), or a higher temperature rise in the coolant. Pumping power can also limit the design window and is discussed below.

Table 2 compares design and operating parameters for the two concepts. The tapered wall allows operation at higher wall loadings with lower pumping power and operating pressures.

Table 2. Design and Operating Parameters Parameters With and Without the Tapered Wall

	Tapered Conducting Wall	Constant Conducting Wall
Wall Thickness at Inlet (cm)	1.5	2
Wall Thickness at Outlet (cm)	0.49	2
Coolant Temperature Rise (K)	200	200
Wall Loading (MW/m^2)	3.8	2.9
Pressure Drop (MPa)	4.3	5.6
Pumping Power (percent thermal)	1.1	1.4
Coolant Velocity (m/s)	0.14	0.10

DESIGN WINDOW SENSITIVITIES

Sensitivity of the design window to the reactor, blanket design, and materials parameters listed in Table 1 have been explored using the above model and are documented in Reference 1. Selected results are presented here in the order in which they appear in the table.

Magnetic field strength obviously has a major impact on pressure drop, and therefore on the design window. Research indicates[7,8,9] that MHD pressure drop is proportional to the square of the magnetic field strength.

Figure 3 shows the design window sensitivity to heated flow path length which is directly related to the tokamak minor radius. The shorter path length blanket can be operated at higher wall loadings with no change in pressure drop or pumping losses. Compact, high beta reactor concepts can reduce both the path length and the magnetic field strength, and therefore are much more promising for self-cooled liquid metal blanket concepts than large tokamaks.

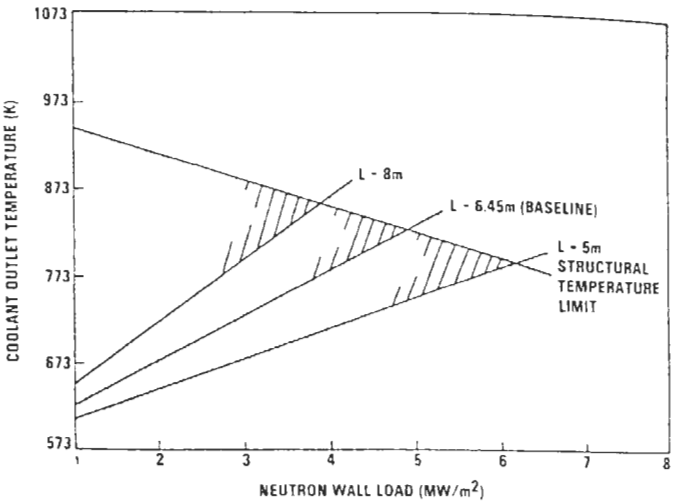

Figure 3. Design Window Sensitivity to Heated Flow Path Length (573 K inlet temperature.)

First wall heat flux effects the temperature and flow requirements at the first wall, and this has a major impact on the design window. Heat transfer at the first wall is discussed below.

Figure 4 shows the design window sensitivity to blanket thickness. Good mixing between the front and back of the blanket is assumed, and no pressure drop penalties for this mixing has been included. Because of the exponential drop-off of heat deposition with depth into the blanket, a thinner blanket receives more heating per unit volume, resulting in a smaller design window.

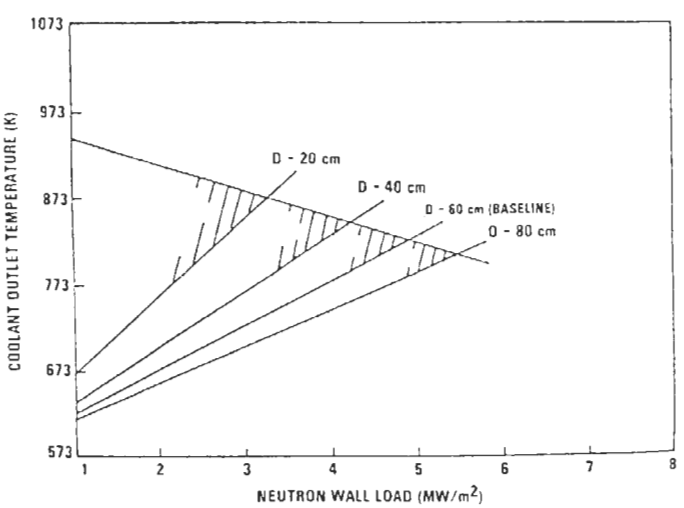

Figure 4. Design Window Sensitivity to Blanket Thickness (Assuming Mixed Flow).

The tapered conducting wall thickness impacts the design window and the pressure drop. Doubling the wall thickness at the inlet to 3 cm (the wall thickness is calculated in the model based on the inlet thickness) increases the maximum wall loading from 4.9 MW/m^2 to 5.2 MW/cm^2, doubles the operating pressure to about 8.4 MPa, and nearly doubles the pumping power. Maximum desired operating pressure and its effects on the tritium breeding ratio limit the wall thickness.

Pumping power may limit the design window, rather than stress, for higher wall thicknesses. Figure 5 shows pumping power limits of 1, 2 and 3 percent for the 3 cm thick wall. Pumping power limits greater than 2 percent do not significantly impact the design window. Note that the pumps required at 2 percent thermal pumping power will use approximately 6 percent of the electric power generated.

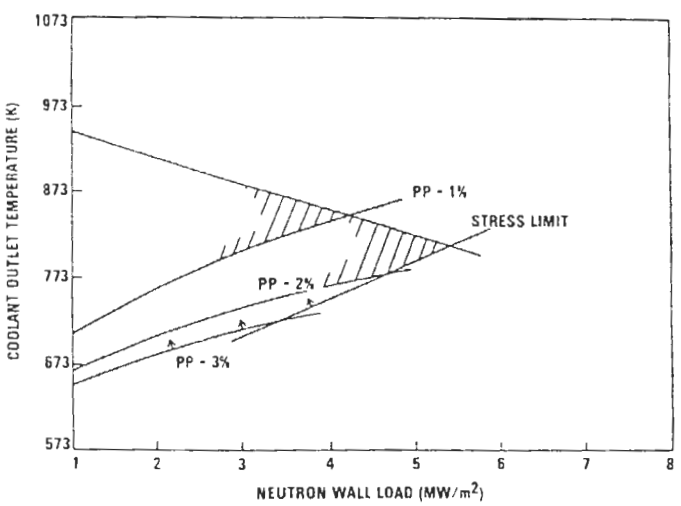

Figure 5. Pumping Power Limits With a Thickness. 3 cm Conducting Wall (573 K inlet temperature).

Maximum and minimum structural temperature limits are set by creep strength, corrosion, liquid metal embrittlement and the ductile to brittle transition temperature. The electrical and thermal conductivities and the maximum allowable primary stress of the structural material also effect the design window. Little data is available on the behavior of materials in a fusion relevant environment, however the available data has been compiled in a consistent manner in the BCSS report.[2] Table 3 lists properties for Vanadium HT-9 and PCA based on those cited in BCSS[2] and Fig. 6 shows the calculated design windows for the three materials. (The effects of varying these properties separately are given in Reference 1.) Properties are assumed to be constant with

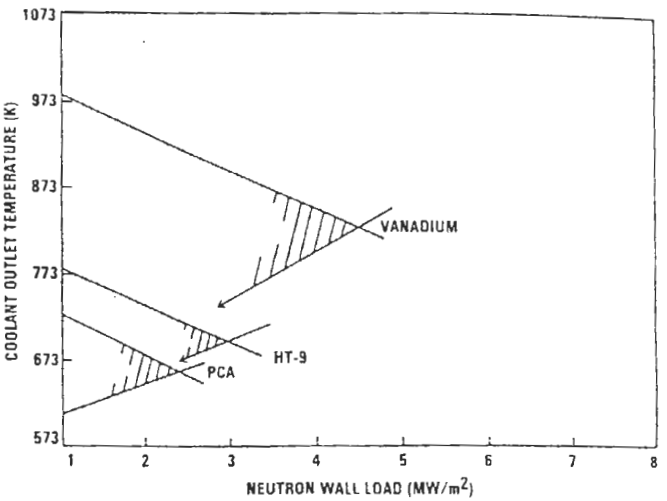

Figure 6. Nominal Design Windows for Vanadium, HT-9 and PCA with Lithium Coolant (573 K inlet temperature).

temperature. The model includes the conduction temperature drop through the first wall. The maximum temperature is limited by the allowable structure temperature, rather than by corrosion, in all three cases. For vanadium, the maximum first wall temperature is 1023 K and the corresponding coolant/structure interface temperature is 941 K, at a neutron wall load of 5 MW/m^2. (Both the film drop and first wall temperature drop are directly proportional to the neutron wall load because the first wall heat flux is assumed to be directly proportional to the neutron wall load.) Unless the corrosion limit is at the low end of the range (923-1023 K in Table 3), the coolant outlet temperature is limited by the structure temperature. The HT-9 and PCA design windows are limited similarly. HT-9 and PCA do not appear to have practical design windows at these reactor parameters unless lower wall loadings become acceptable. The inlet temperature was taken to be 573 K in all three cases, althought PCA is likely to be less susceptible to liquid metal embrittlement and could therefore use a lower inlet temperature.

HEAT TRANSFER AND FLOW DISTRIBUTION

Flow distribution in complex geometries in magnetic fields can strongly affect heat transfer by alternating velocity profiles, and by changing flow rates in parallel channels. In tokamak blankets, high first wall heat fluxes require high coolant velocities, and result in high film temperature

Table 3. Properties and Temperature Limits of Structural Materials Based on Reference 2.

	Vanadium	HT-9	PCA
Max. correction interface temp. range (K)	923-1023	773-873	673-773
Lead-lithium	873-1023	673-773	623-723
Maximum structure temperature (K)	1023	823	773
Maximum allowable (MPa) stress at 100 dpa	155	150	150
Thermal conductivity (W/mK)	25	26	18
Electrical conductivity (10^6/ohm-m)	1.8	?	?

drops. The first wall is the hottest part of the blanket, therefore the film temperature drop must be added to the outlet temperature when determining if maximum allowable temperatures have been met. High film drop temperatures severely reduce the design window.

Figure 7 shows temperature profiles at the outlet of a toroidal first wall channel with slug, parabolic, and Couette velocity profiles, as calculated in Reference 10. The temperature profile through the first wall, including the first wall heat flux and heat generation, is shown on the right, the liquid metal temperature profile is in the area from 5 to 50 mm, and the second wall temperature profile (assuming equal temperatures on either side of the wall) is shown at the left of the figure. Some of the heat deposited in the second wall flows into the channel. The first wall heat flux used in these calculations is 0.7 MW/m^2. The slug velocity profile is Hartmann flow, with no mixing across the channel (laminarized flow). Couette flow is a triangular velocity profile, with the velocity equal to zero at the first wall in this case. Couette flow is intended to model the streaming velocity profiles that can occur in channels parallel to the magnetic field[7]. The results indicate that, to a first order approximation, parabolic flow results in a film temperature drop at the first wall 1.5 times that of Hartmann (or slug) flow, and Couette flow results in a film drop 2.5 times that of Hartmann flow. The Couette flow film drop is extremely high, and may not allow a practical design window.

Hartmann flow is expected to occur in the poloidal channels behind the first wall. Some type of poloidal channel is required to supply liquid metal to the inboard tokamak blanket, therefore the temperature profiles in Hartmann flow in large channels with heat deposition is of general interest. Reference 12 provides an analytic solution for the temperature

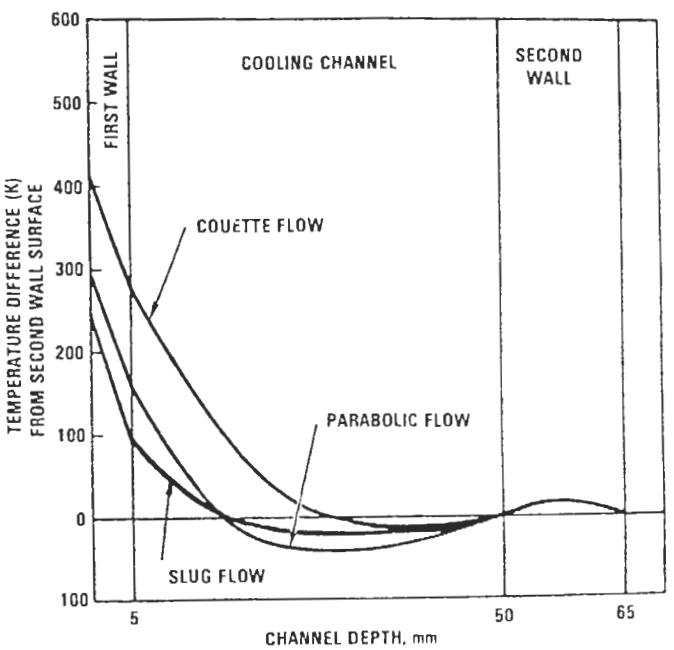

Figure 7. Temperature Profiles at the Outlet of a Toroidal First Wall Channel with Slug, Parabolic, and Couette Velocity Profiles.

profiles in a channel with slug flow, a surface heat flux and an exponential (in space) internal heat generation. The analysis is one dimensional and time dependent, allowing for temperature profile development assuming that the velocity profile is fully developed at the inlet.

Figure 8 shows the temperature profiles in a 55 cm thick, by 6.45 m long, poloidal channel for three cases. Case 1 is the parameters in Table 4, with the above channel dimensions and no wall heat flux. (The front of the poloidal channel is taken at 5 cm behind the first wall to calculate heat generation. Thus, the maximum heat generation

rate in the poloidal channel in Case 1 is 13.75 MW/m^3.) Case 2 is as Case 1 with a 0.1 MW/m^2 heat flux into the channel from the first wall, and Case 3 is as Case 2 with a spatial heat generation decay rate of 4 m^{-1}. The average temperature rise in the channel is 190 K in Cases 2 and 3 and 186 K in Case 1. The film temperature drops are 103 K in Case 1, 175 K in Case 2, and 235 K

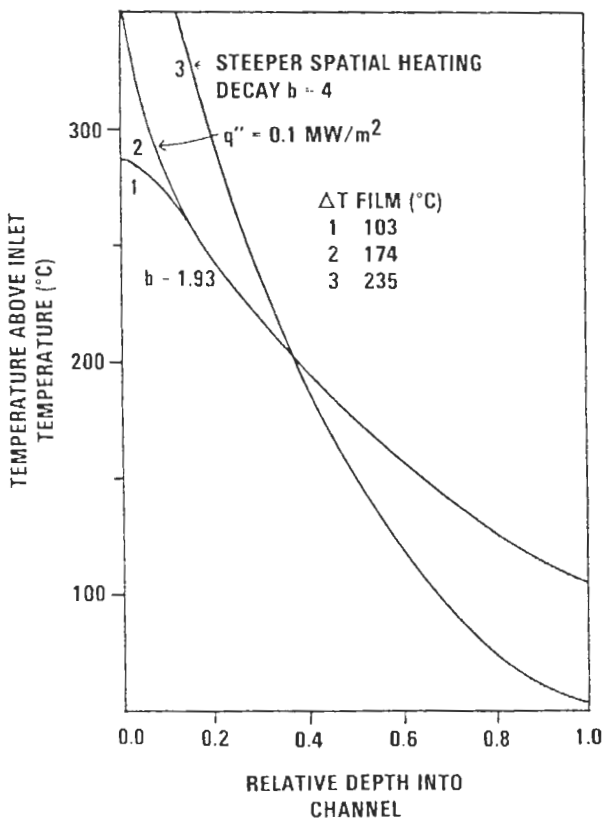

Figure 8. Poloidal Channel Temperature Profiles.

in Case 3. The spatial decay rate of the heating in the bulk blanket is far more important than in the much thinner first wall channels.

Table 4. Parameters used in the Film Film Temperature Drop Calculations

Neutron Wall Load (MW/m^2)	5
Maximum Heat Generation (MW/m^3)	15
First Wall Heat Flux (MW/m^2)	1
Exponential Decay Constant (m^{-1})	1.930
Coolant Velocity (m/s)	1.6
Thermal Conductivity (W/mK)	50
Density (kg/m^3)	470
Heat Capacity (J/kgK)	4180
Channel Depth (cm)	4.5
Channel Length (m)	3

Large temperature gradients in the poloidal channels can present problems due to thermal stress. However, thermal stress can be controlled by proper design. Unless the heat deposition profile is very steep (as in Case 3 in Fig. 8), large front-to-back poloidal channel temperature gradients should not significantly reduce the allowable coolant outlet temperature.

UNCERTAINTIES IN PRESSURE DROP EQUATIONS AND CALCULATION METHODS

Little experimental data exists for MHD pressure drops in complex geometries. Because of the coupling beween vicious and electromagnetic effects, analytic calculations of the pressure drop in relatively simple configurations (e.g., a turn from perpendicular to parallel to the magnetic field) are difficult, and require simplifying assumptions that may or may not be applicable to real situations. The lack of experimental data for verifying theoretical methods has lead to the use of several interpretations and approaches in blanket design studies. In this section, various approaches that have been used in the past are applied to the BCSS toroidal/poloidal flow blanket[6] to understand the range of the uncertainty.

Table 5, adapted from Reference 6, compares pressure drop equations proposed in References 7 and 8. The value of K is determined graphically, and is numerically similar to the values of 0.2 c and c used in the corresponding equations in Reference 7. Thus, these equations are in general agreement when applied to the same situation. However, where and when it is appropriate to apply which equation is not known, and can lead to significant differences in calculated performance.

The equation used for gradually varying magnetic fields in Reference 3 is probably valid as long as the field varies gradually enough that eddy currents and areas of flow stagnation, as accounted for in the equations for varying fields, do not occur. The transition point from one regime to the other is not known. The equation for pressure drop in turns used in Reference 3 yields a significantly lower result that the corresponding equations from the other sources. This is presumably due to the fact that the BCSS toroidal channels are not completely parallel to the field. Turns in the plane perpendicular to the magnetic field are not thought to produce significant pressure drops.[8] However, the behavior in turns from perpendicular to less than parallel is not well understood. In a turn that also invloves a contraction or expansion of the flow, it is not clear whether to use the upstream or the

Applicability	Reference 1,6	Reference 2,9	Reference 5,7
Straight pipe in a transverse magnetic field	$\sigma V B^2 L \frac{c}{1+c}$ (1)	$\sigma V B^2 L \frac{c}{1+c}$	$\sigma V B^2 L \frac{c}{1+c}$
Expansion, contraction fringe fields	$0.2\sigma V B^2 \sqrt{t}\ a$	$K\sigma V B^2 a$	$0.2\sigma V B^2 \sqrt{t}\ a$
Varying field	-	$K\sigma V B^2 a$	$0.2\sigma V B^2 \sqrt{c}\ a$
Gradually varying field	$\sigma V B^2 \left(\frac{1}{r_2} - \frac{1}{r_1}\right) \frac{r_c^2}{1+c}$	-	-
Turn, transverse to longitudinal	-	$K\sigma V B^2 a$	$\sigma V B^2 \sqrt{t}\ a$ (2)
Turn, transverse to nearly longitudinal	$\frac{1}{2} V^{\frac{4}{3}} B^{\frac{4}{3}} \sigma^{\frac{2}{3}} \rho^{\frac{2}{3}} a^{\frac{2}{3}}$	$K\sigma V B^2 a$(?)	$\sigma V B^2 \sqrt{t}\ a$(?)

(1) Equation 9
(2) Equation 14

Table 5. MHD Pressure Drop Equations from Three Sources.

downstream conditions, whether or not to add the expression for a turn and a contraction, or whether the equations listed in Table 5 are applicable at all. Finally, parallel channels are used in several blanket designs, and interactions between electrically connected channels are likely to occur. The impact of these interactions on pressure drop and velocity profiles could be large.

Figure 9 indicates the effect on the design window of applying the equations from Reference 9 (as listed in Table 5) in various interpretations. Table 6 lists the assumptions, in terms of numbers of turns and contractions, used in Fig. 9. Figure 10 shows the geometry schematically. The design window using the values for the pressure drop in the turn and the toroidal channel from BCSS[3] is also shown. The calculations were done as described in Reference 1 and as discussed above. The results indicate a maximum wall loading between 3 and 6 MW/m^2 for a BCSS type tokamak blanket, assuming that the temperature limits are correct. Parallel channel (or other) effects could reduce the worst case wall loading even further. Other permutations of the equations are possible (for example, including terms for fringe effects encountered on entering and exiting the magnetic field), but do not yield significantly differing results.

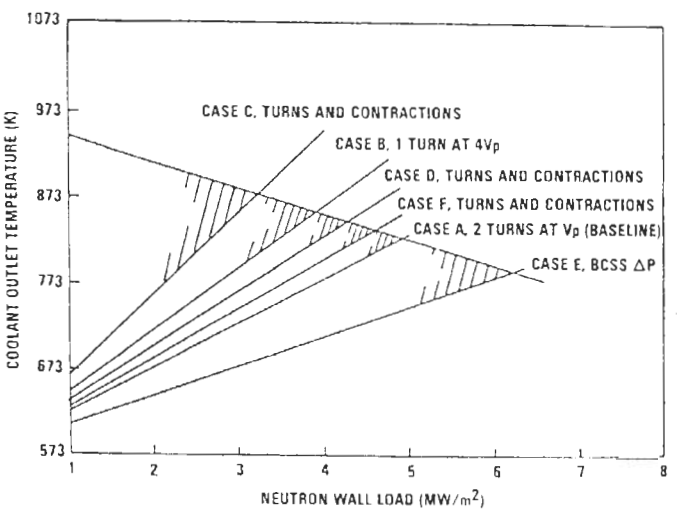

Figure 9. Effect on the Design Window of Assumptions about the Pressure Drop Equations.

POWER CONVERSION EFFICIENCY

The primary coolant inlet and outlet temperatures limit the thermal to mechanical energy conversion efficiency of liquid metal cooled reactors. The second law of thermodynamics tells us that the higher the temperature at which heat is added to a cycle, the higher the efficiency. Both regenerative feedwater heating and reheating increase the average temperature at which heat is added to a Rankine cycle, and therefore increase the efficiency. However, liquid metal cooled fusion reactors are limited by the average primary coolant temperature, and may not be able to take advantage of these methods of increasing efficiency because of pinchpoint problems.

If a certain cycle is chosen, a minimum primary coolant inlet temperature can be determined from the pinchpoint and the primary coolant outlet temperature. However, if the saturation temperature, number of reheats, and amount of regenerative feedwater heating are allowed to vary, lower inlet temperatures are possible by sacrificing efficiency.

Case	A	B	C	D	E	F
Contraction 1	0	0	1	1	0	1
Contraction 2	0	0	4	4	0	1
Expansion 3	0	0	1	1	0	1
Expansion 4	0	0	0.5	0.5	0	0.5
Turn 1	1	4	4	1	*	1
Turn 2	1	0	1	1	0	1
Toroidal Channel	0	0	0	0	*	0

*A pressure drop of 0.41 MPa, from Reference 3, was used for the turn and toroidal channel pressure drop.

Table 6.
Turns and Expansions/Contractions Used in the Cases in Figure 9. Entries in the Table are Multiplied by the Poloidal Channel Velocity and Used in the Equations from Ref. 7 as Listed in Table 5.

A power cycle based on the MARS[4] lead-lithium cycle was used to understand the impcact on efficiency of varying the inlet temperature. The power cycle model uses three stages of feedwater heating, no reheat, and ignores pump losses in the steam cycle. (Liquid metal pumping in included.) The gross efficiency calculated using this model and the MARS parameters is 41.0 percent, which compares well with the 42.0 percent calculated in MARS (for the 900 MWe superheated steam cycle). The operating conditions can be varied to accommodate various coolant inlet and outlet temperatures and steam cycle saturation temperatures and the cycle efficiency can be calculated. (The method and equation are given in Reference 1.) Feedwater heating must be adjusted to allow a reasonable pinchpoint temperature.

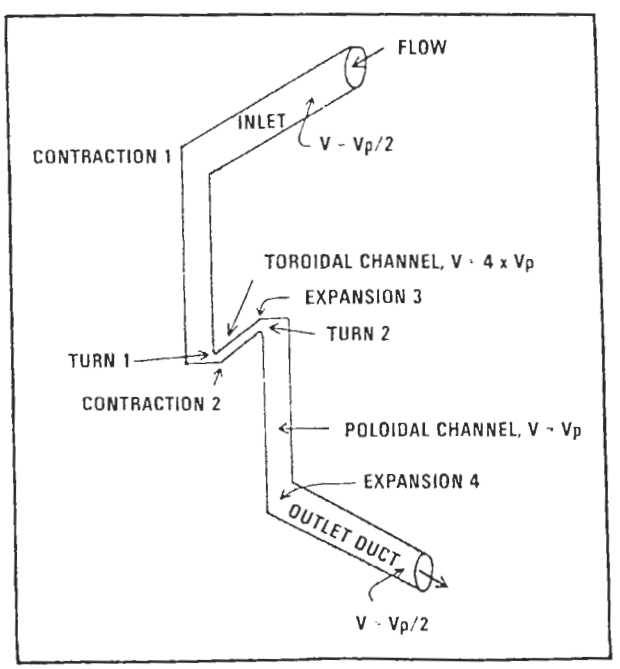

Figure 10. Schematic of the Pressure Drop Models Used in Fig. 9.

Results are given in Fig. 11 for several primary loop inlet temperatures, primary loop outlet temperatures of 723 K, 773 K and 873 K and secondary loop saturation temperatures of 568 K, 603 K and 623 K. The calculated gross efficiency, assuming 90 percent efficiency for all turbines, forms the ordinant. The abcissa is the primary coolant inlet temperature. The pinchpoint temperature difference is held constant at 15 K for all cases. A lower pinchpoint requires a larger heat exchanger (at higher cost) to transfer the same quantity of heat. The upper endpoints of the curves occur where the primary coolant inlet temperature is 15 K (the pinchpoint) above the saturation temperature. At this point, regenerative feedwater heating is used to heat to the saturation temperature. At the opposite (or lower) ends of the curves, no regenerative feedwater heating is used. This point marks the lowest possible primary coolant inlet temperature obtainable at these saturation and outlet temperatures without reducing the pinchpoint temperature. Efficiency is a strong function of inlet temperature and a weaker function of saturation temperature.

As the fraction of regenerative feedwater heating is reduced (and more of the liquid metal heat is used for heating feedwater) the efficiency increases continuously. A point is reached where the third (high temperature) feedwater heater is eliminated entirely, followed by the second and then the first heaters. The knee in the curves occurs at the point where the second (middle temperature) feedwater heater is eliminated.

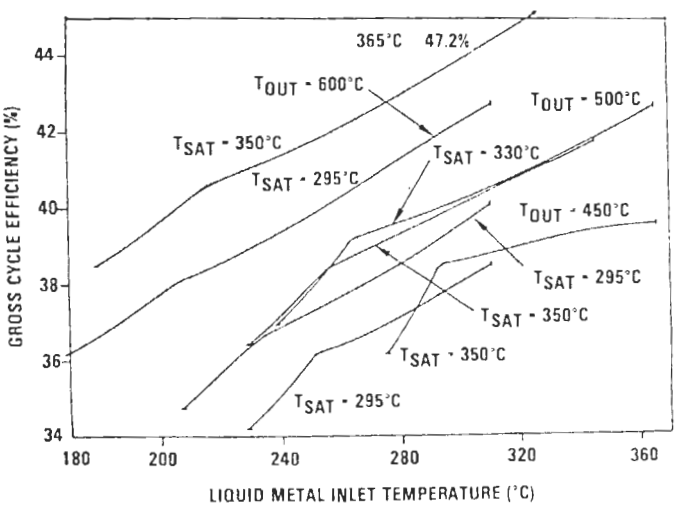

Figure 11. Efficiency Vs Inlet Temperature at Various Outlet and Saturation Temperatures with Variable Feedwater Heating.

Another, less obvious discontinuity also occurs at the point where the first feedwater heater drops out. The large discontinuity is an artifact of the number of feedwater heaters chosen. If very large number of feedwater heaters were used, a continuous curve would be expected along with a somewhat higher efficiency at the highest point. This increased efficiency is bought at an increased cost. Modern power plants often use eight stages of feedwater heating as an optimum. (Reference 13.)

Although our calculations are approximate, it appears that reasonable cycle efficiencies can be obtained for inlet temperatues above 523 K (250 C) and outlet temperatures above 723 K (500 C). Inlet temperatures below 523 K may not be possible because of proximity to the melting point (453 K for lithium and 508 K for lead-lithium) and liquid metal embrittlement, which is most pronounced within 50 to 100 K of the melting point. (Reference 14). Therefore, it appears that minimum liquid metal blanket inlet temperatures will be more limited by parameters other than conversion efficiency or pinchpoint temperature.

CONCLUSIONS

The purpose of the work reported here has been to quantify the uncertainties in the design window for self-cooled liquid metal fusion blankets. Reactor, blanket design, and materials parameters (see Table I contribute to these uncertainties. The size, magnetic fields, and wall loads of a commercial tokamak fusion reactor are not currently well defined. Blanket designs are uncertain because of the unknowns in the other parameters and in MHD phenomena. Irradiated materials properties and structure/coolant interactions, such as liquid metal embrittlement and corrosion, are not well understood. Some fundamental properties, such as the thermal conductivity and heat capacity of lead-lithium, have not been measured. The major uncertainties in the design window arise from the current lack of understanding of MHD phenomena.

Factors that do not appear to be severely limiting now for lithium with vanadium, but which could potentially close or significantly reduce the design window are: corrosion, irradiated material strength and ductility (including DBTT), and liquid metal embrittlement. First wall heat fluxes and/or erosion rates higher than expected could also close the design window, but these present similar problems for other coolants as well.

Figure 12 summarizes the effects of combined uncertainties in the pressure drop, film temperature drop, lower temperature limit and operating pressure limit. The optimistic design window allows neutron wall loads over 6 MW/m^2. The pessimistic window restricts the wall load to under 3 MW/m^2. If the optimistic case is correct, lithium cooled vanadium blankets are very promising. The pessimistic case would probably exclude self-cooled liquid metal blankets for large, high field tokamaks from consideration. Advanced tokamaks, with smaller major radii and lower magnetic fields, will have different numerical limits and different conclusions.

The major differences between the two design windows in Fig. 12 are due to the uncertainties in pressure drop and film temperature drop, as discussed above and in Reference 1. The upper outlet temperature limit line assumes slug flow in the first wall channel and a 2 mm structural first wall thickness. The lower outlet temperature limit line, for the pessimistic window, assumes a parabolic flow profile, resulting in a 67 K higher film temperature drop, and a 3 mm wall, resulting in a 43 K higher temperature drop through the first wall. This results in a significantly steeper outlet temperature limit line for the pessimistic case. The maximum allowable structure temperature (1023 K), rather than corrosion, appears to be the principal outlet temperature limitation for lithium/vanadium. However, the uncertainties in defining the interface temperature are large and may eventually prove to be a serious constraint on the design window.

The lower, upward sloping lines in Fig. 12 are the stress limits due to MHD pressure drop. The major differences between the two windows arise from the number of turns and contractions accounted for in the pressure drop equations, as discussed above. The inlet temperature is 40 K higher in the optimistic case because of LME and/or change in DBTT. Another contributor to the difference in the stress limit lines is that the poloidal channel width in the optimistic case is half that in the pessimistic case. This results in the pressure drop and pumping power being twice as high in the optimistic case if the blanket were operated at a point on the stress limit line. The calculated pressure in the optimistic case is 8.5 MPa, and the pumping power is 2.2% of the thermal power. There is no specific limit on the upper pressure for a liquid metal blanket if the stresses are tolerable, but it may not be desireable to operate at 85 atmospheres.

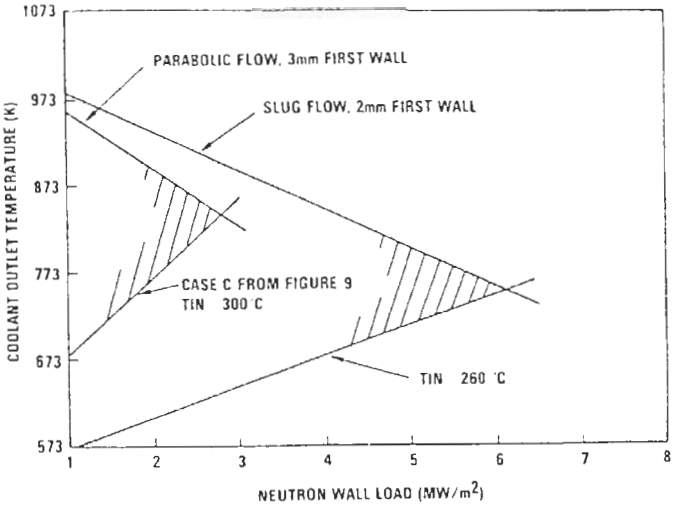

Figure 12. Optimistic and Pessimistic Design Windows for Lithium/Vanadium Considering Uncertainties in Design Optimization, Pressure Drop, Heat Transfer and Temperature Limitations

Determining design window uncertainties cannot be done entirely quantitatively, requiring the frequent use of judgment. Other authors might, therefore, report different numerical values for the possible design windows than those reported here. However, we believe that the following major conclusions will hold.

The major uncertanties in the design window result from uncertainties in MHD pressure drop and film temperature drop. The pressure drop in complex geometries involving turns, parallel channels, expansions and contractions, and flow diagonal to the magnetic field is very poorly understood. This results in an uncertainty factor of between 1.5 and 2 for pressure drop calculations. The flow profile, and therefore the film temperature drop, in regions near turns and contractions or expansions is highly uncertain. A given design could have an uncertainty factor of 2 to 3 or more. If the film drop were high, design changes could probably reduce it significantly, but the final product can not be foreseen. Understanding MHD phenomena sufficiently to determine the practicality of liquid metal blankets will require experiments.

REFERENCES

1. GARNER, J. K., "Uncertainties in Self-Cooled, Liquid Metal Fusion Blanket Design Windows." UCLA-ENG-19, 1985. (Masters thesis.)

2. SMITH, D. L., et al., "Blanket Comparison and Selection Study, Final Report", ANL/FPP-84-1, Argonne National Laboratory, 1984.

3. ABDOU, M. A., et al., "Blanket Comparison and Selection Study, (Interim Report), "ANL/FPP-83-A, Argonne National Laboratory, 1983.

4. LOGAN, B. G., et al., "Mirror Advanced Reactor Study Final Report, "UCRL-53480, Lawrence Livermore National Laboratory, 1984.

5. GARNER, J. K. et al., "A High-Temperature Fusion Blanket for Synfuel and Electrical Production," TANSAO 41 1-712, Transactions of the June, 1982, Annual Meeting of the American Nuclear Society.

6. BERWALD, D. H., et al., "Feasibility Study of a Fission-Supressed Tokamak Fusion Breeder," UCID-20154, Lawrence Livermore National Laboratory, 1984.

7. BADGER, B., et al., "UWMAK-I A Wisconsin Toroidal Fusion Reactor Design, "UWFDM-68, University of Wisconsin, 1974.

8. HUNT, J.C.R. and HOLROYD, R. J., "Applications of Laboratory and Theoretial MHD Duct Flow Studies in Fusion Reactor Technology," CLM-R169, Culham Laboratory, 1977.

9. HOLROYD, R. J. and MITCHELL, J. T. D, "Liquid Lithium as a Coolant for Tokamak Fusion Reactors," CLM-R231, UKAEA, Culham Laboratory, 1982.

10. MADARAME, H., FINESSE project meeting notes, July 1984.

11. ABDOU, M. A., et al., "FINESSE, A Study of the Issues, Experiments and Facilities for Fusion Nuclear Technology Research and Developoment, Interim Report," UCLA-ENG-84-30, University of California, Los Angeles, 1984.

12. LUIKOV, A. V., "Analytical Heat Diffusion Theory," Academic Press, 1968.

13. "Steam, Its Generation and Use" Babcock and Wilcox, 38th Edition, 1972.

14. GORDON, J. D., GARNER, J. K. and HOFFMAN, N. J., "Applications of Lead and Lead-Lithium in Fusion Reactor Blankets", 3rd International Conference on Liquid Metal Engineering in Energy Production, Oxford, 1984.